ELECTRONICS AND ELECTRICAL ENGINEERING
ISSN 1392 – 1215 2011. No. 8(114)
ELEKTRONIKA IR ELEKTROTECHNIKA

HIGH FREQUENCY TECHNOLOGY, MICROWAVES
T 191
AUKŠTŲJŲ DAŽNIŲ TECHNOLOGIJA, MIKROBANGOS

Neural 3-D Smith Chart

M. F. Caglar
Department of Electronics and Communication Engineering, Süleyman Demirel University,
E-9 Building, West Campus, 32260, Isparta, Turkey, phone: 90 246 2111391, e-mail: fatihcaglar@sdu.edu.tr

crossref http://dx.doi.org/10.5755/j01.eee.114.8.700

Introduction

Smith chart is a graphical tool for solving transmission line problems which was developed by P. H. Smith [1]. Every book related on microwave theory or engineering field has had detailed information, solved problems and various applications after its ease of utilization improved on transmission lines [2]. Although analysis and design of microwave circuits are generally tedious with their complicated equations, Smith chart provides a very useful graphical tool or calculator which was improved by computer programmers for these types of the problems with its numerous applications. A microwave engineer having whole concept of the Smith chart in his mind has an ability to picture probable matching solutions for complex problems which includes extensive computation cost.

In the literature, early studies on the computerized Smith chart have been taken place between 1992 and1995 by Prasad and her group in [3–5]. New generation RF/Microwave circuit designers use sophisticated computer-aided design (CAD) tools to decrease the computation time as much as possible. However, the developments in CAD tools do not eliminate the usage Smith chart in design problems. Especially, designers need to consider stability, gain and noise figure circles on a Smith chart for optimum solution options while designing matching networks. Famous design software packages serve design parameters to be figured in a Smith chart plane. Moreover, network analyzers have provided graphical outputs on a Smith chart (e.g. s-parameters applications).

Presenting the negative real half of the impedance values is an important limitation of conventional two-dimensional (2-D) Smith chart. In fact, some oscillator and microwave active filter circuit designs have involved negative resistances. However, it is not practical to manipulate both negative and positive real impedances on the same conventional Smith chart. There is a strong necessity to use separate charts one for the impedances having negative reel part and one for the impedances having positive reel parts. Zelly has proposed to use these two charts side-by-side like a mirror image to easily figure out whole domain in an attempt [6]. Lenzing et al. have suggested using "negative" Smith chart first for designing one-port amplifier [7].

When negative impedances are involved in design, visualizing the Smith chart as a three-dimensional (3-D) sphere rather than a 2-D circle the Smith chart can perform greater insight [6]. Thus, all possible impedances can be performed on the 3-D Smith chart. The power of the 3-D Smith chart has been strengthened with recent studies which are relevant to the theory of the spherical generalized omnipotent Smith charts [8–10]. Besides this, fractional Smith chart is a novel theory to represent fractional order circuit elements as well [11].

The conventional circular Smith chart on a flat 2-D plane has been modeled with Artificial Neural Networks (ANNs) and its impedance matching application in low-noise amplifier (LNA) has been presented [12-13].

In this paper, the 3-D Smith chart has been modeled with ANN to be utilized on the microwave circuitry with the purpose of enough accuracy having fast and practical in-use. Firstly, the mathematical basics of the 3-D Smith chart would have been explained in next section. Then the transformation of the conventional 2-D Smith in order to 3-D spherical Smith chart using ANNs would have been expressed.

The 3-D Smith Chart

In this section, mathematical analysis of spherical 3-D Smith chart has been indicated briefly to get transformation 2-D Smith chart to 3-D Smith chart and numerical computations [8–10]. Initially, the transformation rule between rectangular normalized Z-plane and polar Γ- plane, that is a one-to-one mapping of the resistance and reactance circles as seen in Fig. 1. The transformation rule has been presented as below

$$z = \frac{1+\Gamma}{1-\Gamma} \Leftrightarrow r + jx = \frac{(1+\Gamma_r)+j\Gamma_i}{(1-\Gamma_r)-j\Gamma_i}. \qquad (1)$$

As seen in Fig. 2, two 2-D Smith charts standing side-by-side provides the designer to easily monitor all possible solutions including positive and negative reel part of impedance applications [6, 7].

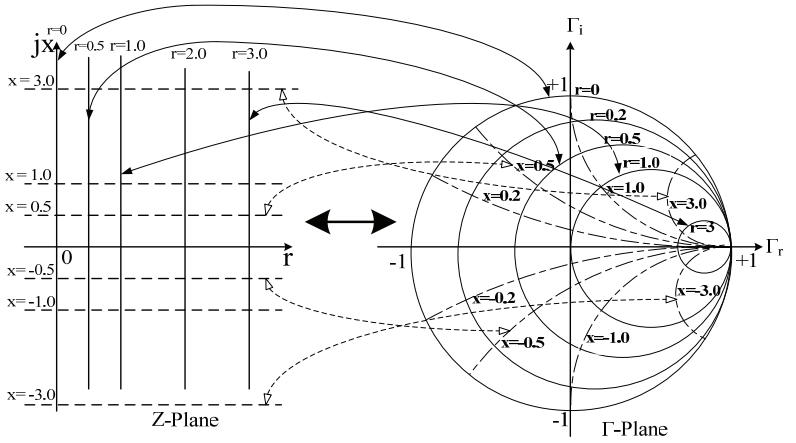

Fig. 1. Resistance (0<r<∞) and reactance (-∞<x<+∞) contours in the impedance and reflection coefficient planes [10]

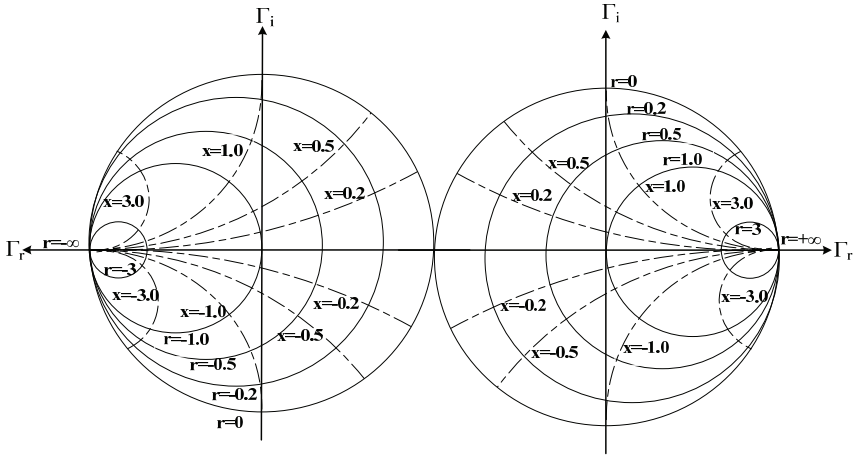

Fig. 2. Side-by-side 2-D Smith chart including resistance (-∞<r<∞) and reactance (-∞<x<+∞) circles

The main idea of joining left-hand side and the right-hand side charts is necessity of overlapping the same circles (also points) like r=0 circles, as given in Fig. 2. Because they are identical and duplication has not been allowed. If the overlapping operation takes place on the 2-D plane, there will be ultimate complexity via mixing positive and negative reel parts.

Zelley has proposed a comprehensible transition way of transforming conventional 2-D Smith chart to 3-D spherical Smith chart without mathematical expressions [6]. Y. Wu et al. have improved mathematical analysis of the 3-D spherical Smith chart [8, 9]. They have introduced two groups of transitions parameters to denote points that generate the resistance and reactance circles on the surface of the unit sphere. The representation of a data point on a resistance or a reactance circle can be developed briefly as follows. Γ_x, Γ_y and Γ_z are the axes of the 3-D Cartesian coordinate system as illustrated in Fig. 3. The points O and A are the centers of the unit sphere and an arbitrary circle on a plane having angular position to Γ_x-Γ_y plane, respectively. The points B, C and D are on the surface of unit sphere and on the circle, too. So the $|BD|$ line defines the diameter of the circle and it's perpendicular to the $|OA|$ line. The two transition parameters are angles which can be defined as $\angle ABO = \varphi$ and $\angle BAC = \theta$. The length of the line $|OB|$=1 and the radius of the arbitrary circle is $|AC|=|AB|=|OB|\cos\varphi=\cos\varphi$. The Γ_y axis value of the point C that is a random selected point on the circle can be obtained as below

$$\Gamma_{yC} = |AC|\sin\theta = \cos\varphi.\sin\theta . \tag{2}$$

The value of Γ_z axis of point C can be obtained via the projection of $|AC|$ to $|AB|$ which is $|AC|_{AB}$:

$$\begin{cases} \Gamma_{zC} = \left(|AB| - |AC|_{AB}\right)\sin\varphi , \\ \Gamma_{zC} = \left(\cos\varphi - \cos\varphi\cos\theta\right)\sin\varphi , \\ \Gamma_{zC} = \sin\varphi\cos\varphi - \sin\varphi\cos\varphi\cos\theta . \end{cases} \tag{3}$$

Similar way to get the Γ_x axis value of C can be tracked:

$$\begin{aligned} &\Gamma_{xC} = |OB| - \left(|AB| - |AC|_{AB}\right)\cos\varphi , \\ &\Gamma_{xC} = 1 - \left(\cos\varphi - \cos\varphi\cos\theta\right)\cos\varphi , \\ &\Gamma_{xC} = 1 - \cos^2\varphi + \cos^2\varphi\cos\theta = \sin^2\varphi + \cos^2\varphi\cos\theta . \end{aligned} \tag{4}$$

All possible points on the surface of the unit sphere can be denoted by using transition parameters which are exactly providing angular intervals in radians as $-\pi<\varphi\leq\pi$ and $-\pi/2\leq\theta\leq\pi/2$. Thus, whole surface of the unit sphere can be scanned by an infinite number of circles.

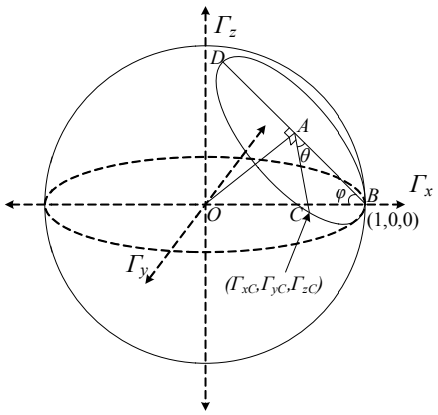

Fig. 3. The 3-D coordinate system of unit sphere

The points that generates resistance and the reactance circles of the spherical 3-D Smith chart is obtained via renaming coordinates $\Gamma_x \rightarrow \Gamma_r$, $\Gamma_y \rightarrow \Gamma_i$, $\Gamma_z \rightarrow \Gamma_z$ for resistance circles and $\Gamma_x \rightarrow \Gamma_r$, $\Gamma_y \rightarrow -\Gamma_z$, $\Gamma_z \rightarrow \Gamma_i$ for reactance circles, respectively. So the coordinates of the r (resistance) points and the x (reactance) points on the surface of the spherical 3-D Smith chart can be defined as follows in (1) and (2), (3), (4) respectively:

$$\begin{cases} \Gamma_r = \sin^2\varphi_r + \cos^2\varphi_r \cos\theta_r \,, \\ \Gamma_i = \cos\varphi_r \sin\theta_r \,, \\ \Gamma_z = \sin\varphi_r \cos\varphi_r - \sin\varphi_r \cos\varphi_r \cos\theta_r \,, \end{cases} \tag{5}$$

$$\begin{cases} \Gamma_r = \sin^2\varphi_x + \cos^2\varphi_x \cos\theta_x \,, \\ \Gamma_i = \sin\varphi_x \cos\varphi_x - \sin\varphi_x \cos\varphi_x \cos\theta_x \,, \\ \Gamma_z = -\cos\varphi_x \sin\theta_x \,. \end{cases} \tag{6}$$

Some r and x circles have been generated in Fig. 4 using (5) and (6) with $-\pi<\varphi\leq\pi$ and $-\pi/2\leq\theta\leq\pi/2$ intervals which blue circles are for x points and red circles are for r points.

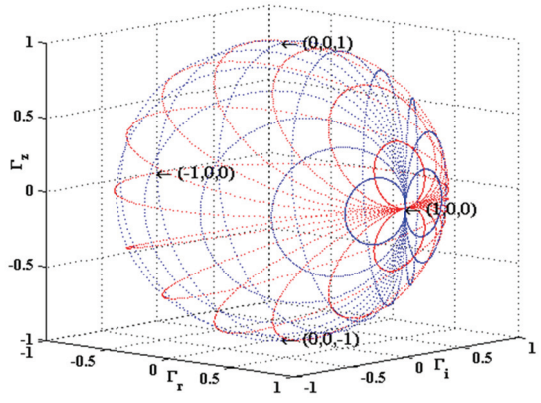

Fig. 4. 3-D Smith chart

At the moment, the most important point is how the relationship can be obtained between conventional 2-D Smith and 3-D Smith chart coordinate system. If Fig. 5 has been examined, the projections of the r and x circles (red and blue ones) of the 3-D Smith chart would have not been overlap the r and x circles of the 2-D conventional Smith chart on the Γ_r-Γ_i plane. So, there is a nonlinear transformation between normalized impedance $z=r+jx$ and transition parameters φ_r, φ_x, θ_r and θ_x. The projection of the diameter $|BD|$ equals to two times of the radius of the concerned resistance circle of the conventional Smith chart on the Γ_r-Γ_i plane as seen in Fig. 3.

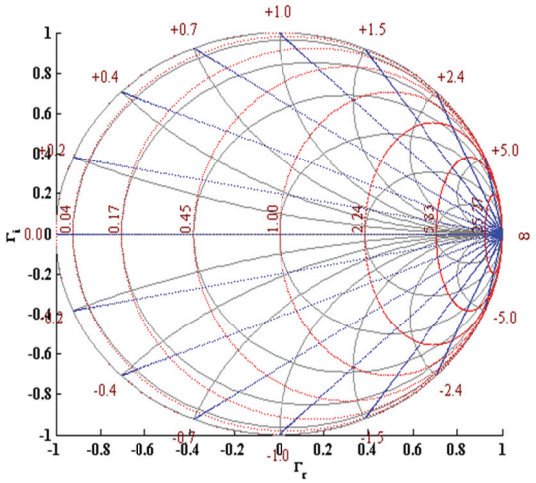

Fig. 5. Resistance and reactance circles of conventional 2-D and 3-D Smith chart

$$\left(\Gamma_r - \frac{r}{r+1}\right)^2 + \Gamma_i^2 = \left(\frac{1}{r+1}\right)^2 . \tag{7}$$

Evaluating this rule and using (7) which has been used for plotting or defining r circles on the 2-D Smith chart the nonlinear relationship between r and φ_r has been obtained as below:

$$\begin{aligned} &|BD|\cos\varphi_r = 2\frac{1}{r+1} \Rightarrow 2\cos\varphi_r \cos\varphi_r = 2\frac{1}{r+1} \,, \\ &\Rightarrow r = \tan^2\varphi_r \,. \end{aligned} \tag{8}$$

The -r (negative r) circles are all on the lower hemi-sphere, so the relationship can be generalized between all possible r circles and φ_r angles as follows:

$$r = \text{sign}(r).\tan^2\varphi_r \,, \tag{9}$$

$$\left(\Gamma_r - 1\right)^2 + \left(\Gamma_i - \frac{1}{x}\right) = \left(\frac{1}{x}\right)^2 . \tag{10}$$

Using similar angular relationships in Fig. 6, the radius of a random oblique circle (P is the center point) on the surface of the spherical Smith chart has been obtained as

$$|KP| = |BP| = |BO|\sin\varphi_x = \sin\varphi_x \,. \tag{11}$$

The diameter of corresponding x circle $|BR|$ on the conventional Smith chart has been presented as follows:

$$\begin{cases} |BR| = \dfrac{|BK|}{\sin\varphi_x} \,, \\ \dfrac{2}{x} = \dfrac{2\cos\varphi_x}{\sin\varphi_x} \,. \end{cases} \tag{12}$$

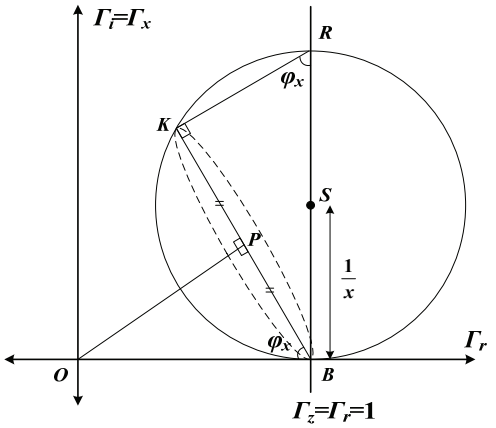

Fig. 6. An random reactance circle a its radius 1/*x*

The nonlinear relationship between all possible *x* circles and φ_x angles can be obtained

$$x = \tan\varphi_x \tag{13}$$

and inverse relationships of (9), (12) and (13) can be obtained as follows:

$$\varphi_r = \frac{1}{2}\operatorname{sign}(r)\arccos\left(\frac{1-|r|}{1+|r|}\right), \tag{14}$$

$$\varphi_x = \arctan x\,. \tag{15}$$

If a point on the surface of the 3-D Smith chart is necessary to be sketched, the parameters θ_r and θ_x would have been needed. It is known that a *z*=*r*+*jx* point has been sketched via *r* and *x* circle intersection on the conventional 2-D Smith chart. Consequently, Γ_r, Γ_i, Γ_z of *r* and *x* circles have been equaled using (5) and (6):

$$\Gamma_r(\varphi_r,\theta_r) = \Gamma_r(\varphi_x,\theta_x),$$
$$\Rightarrow \sin^2\varphi_r + \cos^2\varphi_r\cos\theta_r = \sin^2\varphi_x + \cos^2\varphi_x\cos\theta_x\,, \tag{16}$$

$$\Gamma_i(\varphi_r,\theta_r) = \Gamma_i(\varphi_x,\theta_x),$$
$$\Rightarrow \cos\varphi_r\sin\theta_r = \sin\varphi_x\cos\varphi_x - \sin\varphi_x\cos\varphi_x\cos\theta_x\,, \tag{17}$$

$$\Gamma_z(\varphi_r,\theta_r) = \Gamma_z(\varphi_x,\theta_x),$$
$$\Rightarrow \sin\varphi_r\cos\varphi_r - \sin\varphi_r\cos\varphi_r\cos\theta_r = -\cos\varphi_x\sin\theta_x\,. \tag{18}$$

By omitting $\cos\theta_x$ in (16) and (17) it has been obtained as

$$\theta_r = 2\arctan\left(\frac{1}{\tan\varphi_x.\cos\varphi_r}\right) \tag{19}$$

and by similar approach and omitting $\cos\theta_r$ in (16) and (17) it has been obtained as below

$$\theta_x = -2\arctan\left(\frac{1}{\tan\varphi_r.\cos\varphi_x}\right). \tag{20}$$

As a result, all possible *r* and *x* circles from 2-D Smith chart can be transformed to related *r* and *x* circles on the 3-D Smith chart via equations (14), (15), (19) and (20). The inverse transformation has been possible via equations (9), (12) and (13).

ANN Model of 3-D Smith Chart

The advances in the computational sciences have made nonlinear learning machines possible, which enable to generalize discrete data into the continuous data domain. ANNs are fast and accurate nonlinear learning machines in their matured forms and capable of the parallel processing. Thus, they have found too wide applications in areas of science and engineering. Neural networks are also universal function approximators allowing reuse of the same modeling technology for both linear and nonlinear problems at both device and circuit levels. Neural network models are simple and model evaluation is very fast.

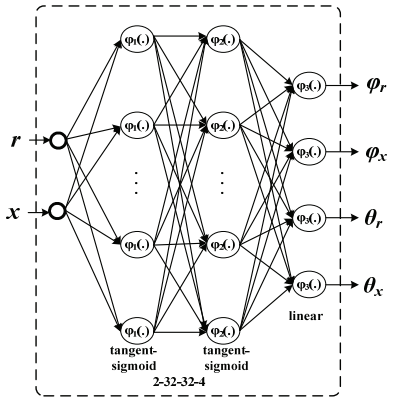

Fig. 7. The architecture of the neural 3-D Smith chart

The ANN architecture of the proposed "Neural 3-D Smith chart" has been demonstrated in Fig. 7. In this architecture, feed-forward Multilayer Perceptron Neural Network (MLPNN) has been used transforming (*r*, *x*) input values to (φ_r, φ_x, θ_r, θ_x) output values. Because the MLPNNs, which have features such as the ability to learn and generalize, smaller training set requirements, fast operation, ease of implementation and therefore most commonly used neural network architectures. The next important concept is how to state the number of hidden layers for this transformation. With this purpose one hidden layer and two hidden layer MLPNNs, both having different number of neurons, have been tried to achieve small training and testing error. Two hidden layer MLPNN is able to learn selected data space more accurate which neurons of the two hidden layers have been activated by tangent-sigmoid function. The output neurons have linear functions for transferring output values of second hidden layer neurons. At last, suitable structure of the MLPNN has been 2-32-32-4.

The input-output data space has been mined using analytical equations (9), (10), (12) and (13) to train and test selected ANN structure. It has been guessed that the training data may be huge, but it must selected an interval for input parameters and it has been prefered an interval as $(r, x) \le |10{,}000|$. By the way, there has been no necessity any interval limitation for output parameters because they have trigonometrical periodicity. The data space has been divided into two parts of 50% training and 50% testing

data. Unless the testing results satisfy, different types of the ANN structures with varied hidden sizes and training algorithms have been tried. A loop has been created to get these trials for best test results.

The Levenberg-Marquardt (LM) back-propagation algorithm for the smallest testing error and four layered network with the minimum number of neuron for faster training have been performed with the MLPNN. The performance function of this network is the Mean Squared Error (MSE). The training convergence of the algorithm is taken place in Fig. 8.

Results

The proposed two hidden layer MLPNN has provided performance with the minimum training error which has been achieved after nearly 400 epochs as 2.45×10^{-5} and average testing error as 4.45×10^{-4}. The MLPNN and the computed (target) output values of the parameters for different r (red holes and stars) and x (blue holes and stars) circles have been given in Fig. 9(a) and Fig. 9(b). The values of the examples have been chosen within the testing data set.

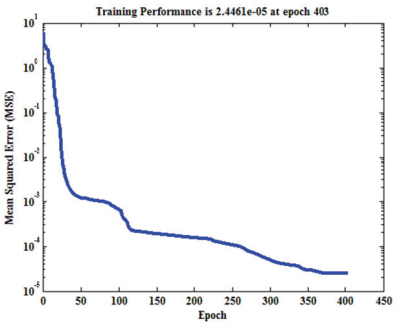

Fig. 8. Training performance of LM backpropagation algorithm

Likewise, an infinite number of arbitrary r and x circles are able to plotted, but the resolution of any figure type doesn't allow. The Tab. 1 has been presented to compensate this leakage. When it has examined, the selected values which are characteristic values of a 2-D Smith chart (e.g. z=±50Ω) and others are extreme to show proof of ANN learning ability satisfy to use "Neural 3-D Smith Chart" in microwave circuitry.

By the way, all computations and manipulations of ANN design have been performed by MATLAB®.

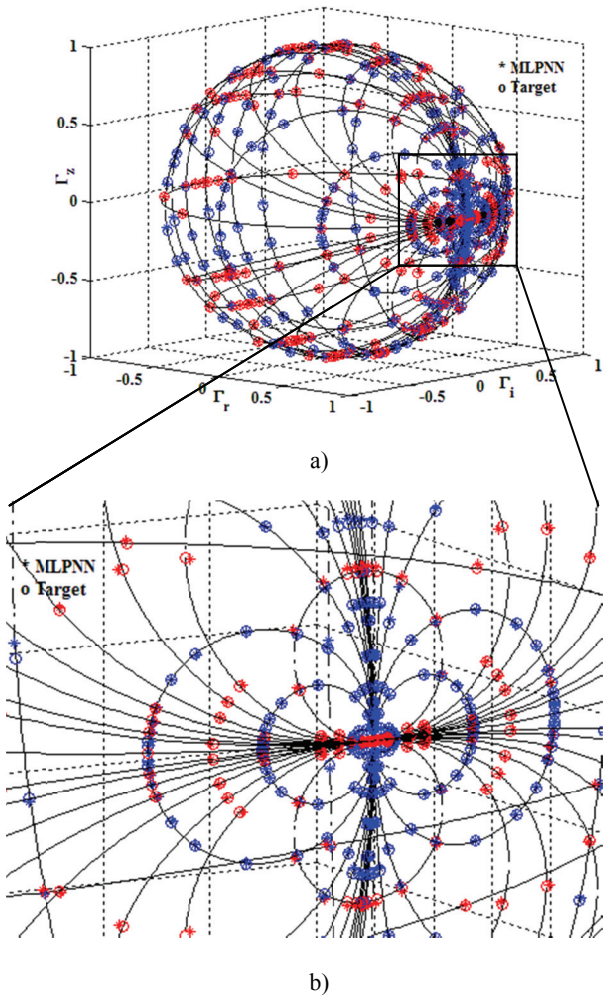

Fig. 9. Comparison of ANN outputs and target data (a) and zooming in of (a) for overlapped data points (b)

Conclusions

The aim of this work is modeling transition relationship from conventional 2-D Smith chart properties to the spherical 3-D Smith chart easily using ANNs. Results on Fig. 9 and test data points on Table 1 has shown that the proposed ANN structure learns all infinite possible points on the surface of the spherical 3-D Smith chart with enough approximation and accuracy.

Table.1. Arbitrary selected examples of ANN outputs and target data for different inputs.

Inputs *(z=r+jx Ω)*→ / Outputs↓		0+j0	1+j0	-1+j0	0.33-j45	-12.23+j0.01	-9019+j7666	-8756-j9898	$(11+j11)10^3$
φ_r (rad.)	ANN	0.0010	0.7861	-0.7860	0.5233	-1.3003	-1.5550	-1.5575	1.5597
	Target	0	0.7854	-0.7854	0.5214	-1.2923	-1.5603	-1.5601	1.5613
φ_x (rad.)	ANN	-0.0002	-0.0002	-0.0001	-1.5490	0.0099	1.5713	-1.5723	1.5701
	Target	0	0	0	-1.5486	0.0100	1.5707	-1.5707	1.5707
θ_r (rad.)	ANN	3.1393	3.1372	3.1395	-0.0550	3.1368	-0.0897	-0.0012	0.0367
	Target	3.1416	3.1416	3.1416	-0.0512	3.1361	0.0248	-0.0189	0.0191
θ_x (rad.)	ANN	-3.1430	-1.5814	1.5824	-3.1103	0.5586	3.0882	3.1370	-3.1149
	Target	-3.1416	-1.5708	1.5708	-3.1161	0.5571	3.1168	3.1227	-3.1225

Consequently, a "Neural 3-D Smith Chart" has been formed by using the ANNs in the simple MLPNN structures as the nonlinear learning machines from the input space to the output space. This novel "Neural 3-D Smith Chart" has been recommended to use in microwave engineering design, especially in some requirements for negative resistances to be used, especially in active filter, oscillator designs and etc. Future studies will involve

applications of microwave engineering designs via "Neural 3-D Smith Chart".

References

1. **Smith P. H.** Transmission line calculator // Electronics, 1939. – Vol. 12. – No.1. – P. 39–42.
2. **Smith P. H.** An improved transmission line calculator // Electronics, 1941. – Vol. 17. – No. 1. – P. 130–133.
3. **Vai M., Prasad S., and Wang, H.** A Smith Chart represented by a neural network and its applications // Microwave Symposium Digest, IEEE MTT–S International, 1992. – P. 1565–1568.
4. **Vai M., Prasad S**. Automatic Impedance Matching with a Neural Network // IEEE Microwave and Guided Wave Letters, IEEE MMT–S, 1993. – Vol. 3. – No. 10. – P. 353–354.
5. **Vai M., Prasad S.,** Microwave circuit analysis and design by a massively distributed computer network // IEEE Microwave Theory and Techniques, IEEE MMT–S 1995. – Vol. 43. – No. 5 – P. 1087–1094.
6. **Zelley C.** A spherical representation of the Smith Chart // IEEE Microwave Magazine, IEEE MMT–S, 2007. – Vol. 8 – P. 60–66.
7. **Lenzing H. F., D'Elio C.** Transmission line parameters with negative conductance loads and the "negative" Smith Chart // Proceedings IEEE, 1963. –Vol. 51. – No. 3. – P. 481–482.
8. **Wu Y., Huang H., Liu Y., Gao Z.** Spherical representation of omnipotent Smith chart // Microwave Optical Technology Letters, IEEE MMT–S, 2008. – Vol. 50. – P. 2452–2455.
9. **Wu Y., Zhang Y., Liu Y., Huang H.,** Theory of the spherical generalized Smith chart // Microwave Optical Technology Letters, IEEE MMT–S, 2009. – Vol. 51. – P. 95–97.
10. **Wu Y., Liu Y., Huang H.,** Extremely generalized planar Smith chart based on Möbius Transformations // Microwave Optical Technology Letters, IEEE MMT–S, 2009. – Vol. 51. – P. 1164–1167.
11. **Shamim A., Radwan A. G., Salama K. N.,** Fractional Smith Chart Theory // IEEE Microwave and Wireless Components Letters, IEEE MMT–S, 2011. – Vol. 21. – No. 3. – P. 117–119.
12. **Güneş F., Çağlar M. F.,** A Novel Neural Smith Chart for Use in Microwave Circuitry // International Journal of RF and Microwave Computer–Aided Engineering. – Wiley InterScience, 2009. – Vol. 19. – Iss. 2. – P. 218–229.
13. **Çağlar M. F., Güneş F.** A 5GHz LNA Design Using Neural Smith Chart // Progress in Electromagnetics Research Symposium (PIERS), 2009. – P. 465–469.

Received 2011 04 28

M. F. Caglar. Neural 3-D Smith Chart // Electronics and Electrical Engineering. – Kaunas: Technologija, 2011. – No. 8(114). – P. 73–78.

In this paper, the three-dimensional (3-D) Smith chart has been modeled with ANN to be utilized on the microwave circuitry with purpose of enough accuracy having fast and practical in-use. Firstly the theory of the 3-D Smith chart has been explained. Then the transformation of conventional 2-D Smith chart to 3-D spherical Smith chart using ANNs has been proposed. Results have shown that proposed ANN structure learns all possible points on the surface of the spherical 3-D Smith chart with enough approximation and accuracy. Consequently, a "Neural 3-D Smith Chart" has been formed by using the ANNs in the simple MLPNN structures as the nonlinear learning machines from the input space to the output space. Ill. 9, bibl. 13, tabl. 1 (in English; abstracts in English and Lithuanian).

M. F. Caglar. Neuroninė trimatė Smito diagrama // Elektronika ir elektrotechnika. – Kaunas: Technologija, 2011. – Nr. 8(114). – P. 73–78.

Analizuojama trimatė Smito diagrama, sudaryta dirbtinių neuroninių tinklų pagrindu. Mikrobangų teorijoje tokia diagrama gali būti taikoma tikslumui padidinti. Pateikiama informacija apie trimates Smito diagramas. Pasiūlytas būdas, kaip, taikant dirbtinius neuroninius tinklus, pereiti iš dvimatės Smito diagramos į trimatę. Nustatyta, kad rezultatai pagerėja, kai mokomi visi galimi sferinio paviršiaus taškai. Il. 9, bibl. 13, lent. 1 (anglų kalba; santraukos anglų ir lietuvių k.).